



## Exciton condensation in strongly correlated quantum spin Hall insulators

A. Amaricci <sup>1</sup>, G. Mazza <sup>2,3</sup>, M. Capone,<sup>4,1</sup> and M. Fabrizio<sup>4</sup>

<sup>1</sup>*CNR-IOM, Istituto Officina dei Materiali, Consiglio Nazionale delle Ricerche, Via Bonomea 265, 34136 Trieste, Italy*

<sup>2</sup>*Dipartimento di Fisica, Università di Pisa, Largo Bruno Pontecorvo 3, 56127, Pisa, Italy*

<sup>3</sup>*Department of Quantum Matter Physics, University of Geneva, Quai Ernest-Ansermet 24, 1211 Geneva, Switzerland*

<sup>4</sup>*Scuola Internazionale Superiore di Studi Avanzati (SISSA), Via Bonomea 265, 34136 Trieste, Italy*



(Received 12 December 2022; revised 6 February 2023; accepted 28 February 2023; published 7 March 2023)

Time-reversal symmetric topological insulators are generically robust with respect to weak local interaction unless symmetry-breaking transitions take place. Using dynamical mean-field theory, we solve an interacting model of quantum spin Hall insulators and show the existence at intermediate coupling of a symmetry-breaking transition to a nontopological insulator characterized by exciton condensation. This transition is of first order. For a larger interaction strength, the insulator evolves into a Mott one. The transition is continuous if magnetic order is prevented, and notably, for any finite Hund's exchange, it progresses through a Mott localization before the condensate coherence is lost. We show that the correlated excitonic state corresponds to a magneto-electric insulator, which allows for direct experimental probing. Finally, we discuss the fate of the helical edge modes across the excitonic transition.

DOI: [10.1103/PhysRevB.107.115117](https://doi.org/10.1103/PhysRevB.107.115117)

The concept of symmetry protected topology has introduced a new paradigm for the description of electronic band structures [1,2]. The early identification of topological states in semiconducting quantum wells [3,4] and three-dimensional chalcogenides [5–8] boosted intense research activity that finally reached a mature symmetry groups classification for weakly interacting insulators and semimetals. The discovery of topological properties in more correlated materials [9,10], such as monolayers of early transition-metal dichalcogenides (TMDs) [11–13] or some Fe-based compounds [14–18], raised interest in the role of the ever-present electron-electron interaction in topological phases of matter.

The electron localization tendency brought in by strong correlations can generically lead to dramatic modifications of the band-structure topology [19]. Contrary to naive expectations, Coulomb repulsion can, in some cases, favor the formation of a nontrivial electronic state [10,20], trigger the existence of novel purely interacting topological phases [21], or drive a dynamical change in the thermodynamic character of the topological quantum phase transition [22–25]. Yet, the most impactful effect of strong electronic correlations is often the emergence of ordered phases. At strong coupling, the existence of large spin exchanges and spin-orbit coupling paves the way to magnetically ordered states. For weaker interaction strength, the situation can get more intriguing since diverse degrees of freedom are equally active and possibly cooperate with the nontrivial topology of the electronic bands. In these conditions, different instabilities compete, and it becomes hard to predict the electronic properties of a correlated topological insulator.

One of the most interesting effects of electronic interaction in systems hosting a small energy gap is to induce in-gap excitons [26–32]. Although excitons have been studied for long, recent evidence supporting the existence of excitonic phases in TMD monolayers [11–13,33] gave a strong impulse to the

investigation of excitons in topological insulators [26,28,30]. For instance, the anomalies observed in the topological Kondo insulator  $\text{SmB}_6$  have been predicted to be caused just by excitons [34–38].

Here, we show that exciton phase transition generically occurs due to electronic correlations in a model quantum spin Hall insulator (QSHI). In particular, using a nonperturbative approach based on dynamical mean-field theory (DMFT) [39–41], we demonstrate that, in the presence of a sufficiently strong interaction, the QSHI becomes unstable towards an excitonic phase with an in-plane spin polarization [28,42] that breaks the time-reversal, spin  $U(1)$ , and parity symmetries [30] that protect topological order. The transition between the QSHI and the excitonic insulator (EI) is of first order within DMFT. The excitonic phase shows a finite magnetoelectric susceptibility [43,44], which allows a direct experimental identification of such a state of matter.

The rest of the paper is organized as follows. In Sec. I, we introduce the interacting QSHI model and briefly recall the method used to solve it. In the following Sec. II, we discuss the excitonic phase transitions occurring for generic values of the parameters, distinguishing the two cases corresponding to the presence or the absence of Hund's exchange. We summarize part of the findings in terms of the phase diagram in Sec. III. In Sec. IV we discuss observable consequences of the excitonic transition in the QSHI. Finally, in Sec. V, we draw the conclusions of our paper and discuss some perspectives.

### I. MODEL AND METHODS

We consider an interacting two-orbital Hubbard model on a two-dimensional square lattice [3,22], described by the Hamiltonian,

$$H = \sum_{\mathbf{k}} \psi_{\mathbf{k}}^{\dagger} H(\mathbf{k}) \psi_{\mathbf{k}} + H_{\text{int}}, \quad (1)$$

with the spinor  $\psi_{\mathbf{k}}^\dagger = [c_{\mathbf{k}1\uparrow}^\dagger, c_{\mathbf{k}2\uparrow}^\dagger, c_{\mathbf{k}1\downarrow}^\dagger, c_{\mathbf{k}2\downarrow}^\dagger]$  and where  $c_{\mathbf{k}\alpha\sigma}^\dagger$  creates an electron on orbital  $\alpha = 1, 2$  with spin  $\sigma = \uparrow, \downarrow$  at momentum  $\mathbf{k}$ . Orbitals 1 and 2 transform as the  $\ell = 0$  and  $\ell = 1$  spherical harmonics, respectively [3], and, more specifically,

$$(2, \uparrow) \equiv (\ell = 1, \ell_z = +1, \uparrow),$$

$$(2, \downarrow) \equiv (\ell = 1, \ell_z = -1, \downarrow)$$

are the  $j_z = \pm 3/2$  components of  $j = 3/2$  spin-orbit multiplet.

We introduce the  $4 \times 4$  matrix basis  $\Gamma_{\alpha\alpha} = \sigma_\alpha \otimes \tau_\alpha$ , where  $\sigma_{\alpha=0-3}$  and  $\tau_{\alpha=0-3}$  are Pauli matrices, including the identity, in spin, and orbital subspaces, respectively. The noninteracting Hamiltonian matrix reads

$$H(\mathbf{k}) = M(\mathbf{k})\Gamma_{03} + \lambda \sin(k_x)\Gamma_{31} - \lambda \sin(k_y)\Gamma_{02}, \quad (2)$$

where  $M(\mathbf{k}) = M - \epsilon(\cos k_x + \cos k_y)$ ,  $M \geq 0$  being the energy separation between the two orbitals,  $\epsilon$  is the hopping amplitude, and  $\lambda$  is the interorbital hybridization that lacks an on-site component because of inversion symmetry. Hereafter, we take  $\epsilon = 1$  as our unit of energy  $\lambda = 0.3$  and assume two electrons per site, i.e., half-filling. The noninteracting Hamiltonian is invariant under time reversal symmetry  $\mathcal{T}$ , inversion symmetry  $\mathcal{P}$ ,  $U(1)$  spin rotations around the  $z$  axis, and the fourfold  $C_4$  spatial rotations around  $z$ . Any space-isotropic and spin- $SU(2)$  symmetric two-body potential projected onto the local basis set inevitably yields interaction terms that are only invariant under inversion and spin  $U(1)$ . Here, we assume the local interaction,

$$H_{\text{int}} = \frac{1}{4} \sum_{\mathbf{r}} (2U - 3J)\hat{N}_{\mathbf{r}}^2 - J\hat{S}_{\mathbf{r}}^2 + 2J\hat{T}_{\mathbf{r}}^2, \quad (3)$$

where the operators,

$$\hat{N}_{\mathbf{r}} = \psi_{\mathbf{r}}^\dagger \Gamma_{00} \psi_{\mathbf{r}}, \quad \hat{S}_{\mathbf{r}} = \frac{1}{2} \psi_{\mathbf{r}}^\dagger \Gamma_{30} \psi_{\mathbf{r}}, \quad \hat{T}_{\mathbf{r}} = \frac{1}{2} \psi_{\mathbf{r}}^\dagger \Gamma_{03} \psi_{\mathbf{r}},$$

with  $\psi_{\mathbf{r}}$  as the Fourier transform of  $\psi_{\mathbf{k}}$ , are, respectively, the density, the spin polarization along  $z$ , and the orbital polarization at lattice site  $\mathbf{r}$ . The interaction (3) enforces Hund's first rule of maximum spin. However, it is not the most general symmetry-allowed one [30], which may also include the pair-hopping process  $c_{\mathbf{r}1\uparrow}^\dagger c_{\mathbf{r}1\downarrow}^\dagger c_{\mathbf{r}2\downarrow} c_{\mathbf{r}2\uparrow} + \text{H.c.}$ . This term opposes against Hund's first rule, but, physically, cannot prevail over the latter. Therefore, neglecting pair-hopping processes as we do in Eq. (3) is not expected to qualitatively alter the physics but has the great advantage of making the interaction much easier to deal with numerically.

We solve the model nonperturbatively by single-site DMFT [39]. Within DMFT, the self-energy is approximated by a momentum-independent but frequency-dependent matrix function in spin and orbital space, which is obtained from the solution of an effective quantum impurity problem, which we address using the exact diagonalization method. In this approach, the effective bath is discretized in terms of  $N_b$  levels. The low-energy spectrum and the zero-temperature dynamical correlation functions of the impurity Hamiltonian are obtained using a Lanczos-based algorithm. More details can be found in Ref. [45]. In this paper, we used  $N_b = 8$  and checked the stability of the solution with respect to  $N_b$  for selected values of the model parameters. A symmetry-invariant self-energy matrix is diagonal with spin-independent elements.

Deviations from such a matrix structure signal the onset of symmetry breaking [24,28,42,46–50]. The noninteracting model has a topological quantum phase transition between a QSHI for  $M < 2$  and a trivial band insulator (BI) for  $M > 2$ . In the presence of a finite Hund's exchange  $J$  and for large  $U$ , see Eq. (3), a high-spin Mott insulator sets in [22,49,51] and describes two electrons localized on each site and forming a spin  $S_z = \pm 1$  configuration, thus, with vanishing orbital polarization  $T_z = 0$ .

## II. THE EXCITONIC PHASE TRANSITION

In order to assess the possible instability of the model towards an excitonic phase, it is instructive to start from the atomic limit with two electrons per site. The Hamiltonian in the two-electron subspace reads

$$H_{\text{at}} = \sum_{\mathbf{r}} -J\hat{S}_{\mathbf{r}}^2 + 2J\hat{T}_{\mathbf{r}}^2 + 2M\hat{T}_{\mathbf{r}}.$$

The eigenstates can be labeled by the eigenvalues  $S_z$ ,  $T_z$ , and  $\ell_z$ , respectively, of the operators  $\hat{S}_{\mathbf{r}}$ ,  $\hat{T}_{\mathbf{r}}$ , and

$$\hat{\ell}_z = n_{2\uparrow\mathbf{r}} - n_{2\downarrow\mathbf{r}},$$

with  $n_{\alpha\sigma\mathbf{r}} = c_{\alpha\sigma\mathbf{r}}^\dagger c_{\alpha\sigma\mathbf{r}}$ . Thus, the states  $|(\ell_z, S_z, T_z), \mathbf{r}\rangle$  have eigenvalues  $E(\ell_z, S_z, T_z)$ ,

$$E(0, 0, +1) = 2J + 2M,$$

$$E(0, 0, -1) = 2J - 2M,$$

$$E(+1, +1, 0) = E(-1, -1, 0) = -J,$$

$$E(+1, 0, 0) = E(-1, 0, 0) = 0. \quad (4)$$

For  $3J > 2M$ , the atomic ground state is the high-spin doublet with  $S_z = \pm 1$ , otherwise is state  $|(0, 0, -1), \mathbf{r}\rangle$  with two electrons in orbital 2. Our aim is to study the competition between those states, and, therefore, we hereafter drop the other three states,  $|(0, 0, +1), \mathbf{r}\rangle$  and  $|(\pm 1, 0, 0), \mathbf{r}\rangle$ .

Moreover, we define a pseudospin operator  $\mathbf{I}_{\mathbf{r}} = (I_{x\mathbf{r}}, I_{y\mathbf{r}}, I_{z\mathbf{r}})$  through

$$I_{z,\mathbf{r}}|(+1, +1, 0), \mathbf{r}\rangle \equiv |z| + 1, \mathbf{r}\rangle = | +1, \mathbf{r}\rangle,$$

$$I_{z,\mathbf{r}}|(0, 0, -1), \mathbf{r}\rangle \equiv |z|_0, \mathbf{r}\rangle = 0,$$

$$I_{z,\mathbf{r}}|(-1, -1, 0), \mathbf{r}\rangle \equiv |z| - 1, \mathbf{r}\rangle = -| -1, \mathbf{r}\rangle,$$

so that the three states become the components of an  $I = 1$  pseudospin. In this subspace, the following equivalences hold

$$\psi_{\mathbf{r}}^\dagger \Gamma_{11} \psi_{\mathbf{r}} \equiv \sqrt{2}I_{x\mathbf{r}},$$

$$\psi_{\mathbf{r}}^\dagger \Gamma_{21} \psi_{\mathbf{r}} \equiv \sqrt{2}I_{y\mathbf{r}},$$

$$\psi_{\mathbf{r}}^\dagger \Gamma_{12} \psi_{\mathbf{r}} \equiv -\sqrt{2}[I_{y\mathbf{r}}, I_{z\mathbf{r}}]_+,$$

$$\psi_{\mathbf{r}}^\dagger \Gamma_{22} \psi_{\mathbf{r}} \equiv -\sqrt{2}[I_{x\mathbf{r}}, I_{z\mathbf{r}}]_+,$$

$$\psi_{\mathbf{r}}^\dagger \Gamma_{03} \psi_{\mathbf{r}} \equiv 2(1 - I_{z\mathbf{r}}^2),$$

$$\psi_{\mathbf{r}}^\dagger \Gamma_{30} \psi_{\mathbf{r}} \equiv 2I_{z\mathbf{r}},$$

whereas  $\psi_{\mathbf{r}}^\dagger \Gamma_{\alpha\alpha} \psi_{\mathbf{r}}$  with all other  $\Gamma$  matrices different from the identity have vanishing matrix elements.

The atomic Hamiltonian projected onto the subspace  $|0, \mathbf{r}\rangle$  and  $|\pm 1, \mathbf{r}\rangle$  becomes, dropping constants,

$$H_{\text{at}} \simeq \Delta E \sum_{\mathbf{r}} (1 - I_{z\mathbf{r}}^2), \quad \Delta E = 3J - 2M.$$

Our interest is studying how the hopping processes beyond the atomic limit modify the level crossing between  $|\pm 1, \mathbf{r}\rangle$

and  $|0, \mathbf{r}\rangle$  when  $\Delta E$  changes sign. For that, we treat those processes at second order in perturbation theory and, after projection onto the above subspace, we find an effective Heisenberg Hamiltonian for the  $I = 1$  pseudospins,

$$\begin{aligned}
 H_* = \Delta E_* \sum_{\mathbf{r}} (1 - I_{z\mathbf{r}}^2) \\
 + J_+ \sum_{\langle \mathbf{r}\mathbf{r}' \rangle} \left( 2I_{z\mathbf{r}}I_{z\mathbf{r}'} - \sum_{a=x,y} I_{a\mathbf{r}}I_{a\mathbf{r}'} \right) \\
 + J_- \sum_{\langle \mathbf{r}\mathbf{r}' \rangle} \left( K_{z\mathbf{r}}K_{z\mathbf{r}'} - \sum_{a=x,y} K_{a\mathbf{r}}K_{a\mathbf{r}'} \right), \quad (5)
 \end{aligned}$$

where  $K_{a\mathbf{r}} = I_{a\mathbf{r}}I_{z\mathbf{r}} + I_{z\mathbf{r}}I_{a\mathbf{r}}$ , whereas

$$\Delta E_* = \Delta E + 8J_-, \quad J_{\pm} = \frac{1 \pm \lambda^2}{4U}.$$

When  $\Delta E_* \gg J_+ > J_-$ , the ground state is a Néel antiferromagnet with  $\langle I_{z\mathbf{r}} \rangle = (-1)^{\mathbf{r}}$ . On the contrary, when  $\Delta E_* \ll -|J_+|$ , each site in the ground state is locked into the  $I_z = 0$  eigenstate of the pseudospin triplet, which is just the trivial band insulator since the topological one does not survive in the atomic limit. These two states might cross in energy when  $\Delta E_* \simeq 0$ , but that crossing is avoided by the quantum fluctuations brought about by  $J_+$  and  $J_-$  that, in turn, compete against each other favoring mutually exclusive symmetry-breaking routes. Presumably, the system chooses the route with largest coupling constant, i.e.,  $J_+$ . Therefore, since our aim is just to infer the physical behavior of the Hamiltonian (5) without pretending to get any quantitative result, we can safely neglect  $J_-$ . In that case, the Hamiltonian (5) describes an easy-axis XXZ Heisenberg model with a single-ion anisotropy  $\Delta E_*$ , which suggests that the transition between the Néel antiferromagnet and the band insulator might occur through an intermediate phase characterized by the order parameter,

$$\begin{aligned}
 \Delta(\phi) = \langle I_{x\mathbf{r}} + I_{y\mathbf{r}} \rangle = \frac{1}{\sqrt{2}} \langle \psi_{\mathbf{r}}^\dagger (\Gamma_{11} + \Gamma_{21}) \psi_{\mathbf{r}} \rangle \\
 \equiv \Delta_{11} + \Delta_{21} = \Delta \cos(\phi) + \Delta \sin(\phi), \quad (6)
 \end{aligned}$$

which breaks  $\mathcal{T}$ , inversion-symmetry  $\mathcal{P}$ , and spin  $U(1)$  symmetry for any fixed value of  $\phi \in [0, 2\pi)$  [30]. This phase actually describes a condensate of odd-parity spin-triplet excitons with the spin lying on the  $x$ - $y$  plane.

To assess whether such excitonic phase indeed exists and does survive at intermediate coupling, we have calculated the dynamical susceptibility  $\chi_{11}^{\text{imp}}(\omega) = \frac{1}{N} \int dt e^{i\omega t} \langle T_t [\Gamma_{11}(t) \Gamma_{11}(0)] \rangle$  forcing all symmetries within the effective impurity problem of the DMFT [39] and where  $\Gamma_{\alpha\alpha} = \psi^\dagger \Gamma_{\alpha\alpha} \psi$  [28,30] are impurity operators. Although this quantity does not necessarily correspond to the local susceptibility of the bulk model, nonetheless, it provides suitable information about its instabilities. In Fig. 1, we report the evolution of  $\chi_{11}^{\text{imp}}(\omega)$ , which is equivalent to  $\chi_{21}^{\text{imp}}(\omega)$  by spin  $U(1)$  symmetry as a function of energies  $\omega$  and  $U$  at  $M = 3.5$ , thus, along the path from the band to the Mott insulator. In the weakly interacting regime, this function displays several high-energy peaks. Increasing  $U$  leads to redshift of the lowest-energy peak until it softens before the

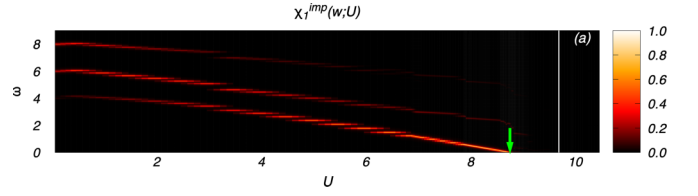


FIG. 1. Evolution of the low-energy spectra of the in-plane triplet component of the exciton-exciton susceptibility  $\chi_1^{\text{imp}}(\omega)$  as a function of the interaction strength  $U$ . Data for  $J/U = 0.25$  and  $M = 3.5$ . The arrow indicate the softening of the lowest-energy peak before the Mott insulator sets in (white solid line).

Mott transition sets in. The softening is just the signal of the excitonic instability.

However, the conclusive proof of excitonic transition can be obtained allowing for symmetry breaking, which we do though forcing for simplicity, translational symmetry. Our results are reported in Fig. 2 for  $J = 0.25U$ , left panel, and  $J = 0$ , right panel.

### A. The $J > 0$ case

For any  $M > 0$ 's, we observe the formation of an EI with

$$P_1 = \langle \psi_{\mathbf{r}}^\dagger \Gamma_{11} \psi_{\mathbf{r}} \rangle \neq 0,$$

which is related to  $\langle \psi_{\mathbf{r}}^\dagger \Gamma_{21} \psi_{\mathbf{r}} \rangle$  under spin  $U(1)$ , see Eq. (6). The transition from the band or topological insulators to the excitonic one is of first order, whereas that from the EI to the high-spin Mott insulator (hs-MI) is of second order. We cannot exclude that also the latter transition may become first order allowing for translational symmetry breaking, and, thus, for an antiferromagnetic Mott insulator [24].

The order parameter  $P_1$  as a function of  $U$  displays a bell-like structure, which is centered at increasing values of  $U$  as  $M$  grows. Interestingly, the peak value is attained at different positions depending on the nature of the uncorrelated insulator. For  $M < 2$  (QSHI) the peak value is reached immediately after the transition whereas for  $M > 2$  (BI) the peak is well inside the excitonic region. We also observe that the orbital

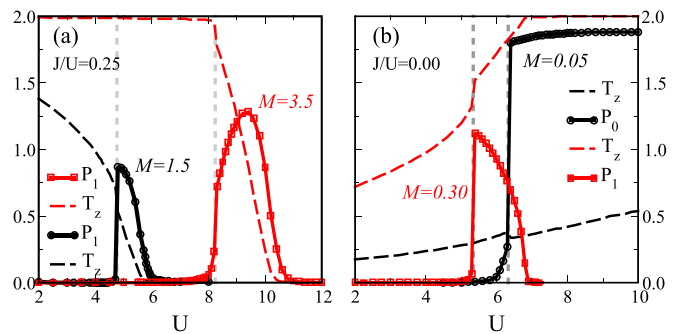


FIG. 2. Orbital polarization  $T_z$  (dashed lines) and exciton-order parameter  $P_1$  (solid line and symbols) as a function of the interaction strength  $U$  at  $J = 0.25U$ , left panel, and  $J = 0$ . For the  $J = 0$  case, we also show the order-parameter  $P_0$  corresponding to the formation of an odd-parity spin-singlet excitonic state, which is always zero at  $J = 0.25U$ .

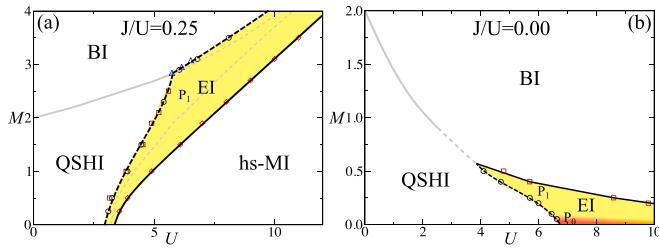


FIG. 3. DMFT phase diagrams of the interacting model as a function of  $U$  and  $M$ . Left panel (a) for  $J/U = 0.25$ . Right panel (b) for  $J = 0$ . The nature of the leading excitonic-order parameter is indicated in the plot using text and color code. First-order transitions are indicated with dashed lines. Continuous transitions are indicated with solid lines. Transitions to/from EI are indicated in black. Gray lines in the background indicate the transitions occurring without allowing for exciton condensation.

polarization  $T_z$  vanishes before the Mott transition, i.e., when  $P_1$  is still finite.

### B. The $J = 0$ case

At  $J = 0$ , the atomic levels (4) include the ground-state  $|0, 0, -1\rangle$ , followed at energy  $2M$  above by the fourfold multiplet  $|\pm 1, \pm 1, 0\rangle$  and  $|\pm 1, 0, 0\rangle$ , and, finally, by  $|0, 0, +1\rangle$  at energy  $4M$  above the ground state. For large  $U$ , the hopping at second order in perturbation theory generates superexchange processes of order  $1/U$ . Therefore, the model at  $U \rightarrow \infty$  and finite  $M$  describes just the band insulator with two electrons in orbital 2. However, the situation may change if  $M$  scales as  $1/U$ . In that case, and if we discard the highest-energy atomic level  $|0, 0, +1\rangle$ , the superexchange processes mix the atomic ground-state  $|0, 0, -1\rangle$  with the first excited multiplet on nearest-neighbor sites. Similar to the  $J > 0$  case, these processes may lead to finite expectation values of the local operators that have finite matrix elements between the  $|0, 0, -1\rangle$  and the fourfold multiplet  $|\pm 1, \pm 1, 0\rangle \oplus |\pm 1, 0, 0\rangle$ . We already showed that at  $\lambda \neq 0$  the mixing between  $|0, 0, -1\rangle$  and the doublet  $|+1, +1, 0\rangle \oplus |-1, -1, 0\rangle$  stabilizes the order parameters  $P_1 = \langle \psi_{\mathbf{r}}^\dagger \Gamma_{11} \psi_{\mathbf{r}} \rangle$  and its spin- $U(1)$  partner  $\langle \psi_{\mathbf{r}}^\dagger \Gamma_{21} \psi_{\mathbf{r}} \rangle$ .

Similarly, the order parameters  $P_0 = \langle \psi_{\mathbf{r}}^\dagger \Gamma_{01} \psi_{\mathbf{r}} \rangle$  and its  $C_4$  partner  $\langle \psi_{\mathbf{r}}^\dagger \Gamma_{32} \psi_{\mathbf{r}} \rangle$ , which, thus, break  $C_4$  and inversion symmetries, are favored by the mixing between  $|0, 0, -1\rangle$  and doublet  $|+1, 0, 0\rangle \oplus |-1, 0, 0\rangle$  at  $\lambda \neq 0$ .

Our explicit DMFT calculations predict that, at  $M \sim 1/U$ ,  $P_1$  is always stabilized except at very small  $M$ , where the order parameter  $P_0$  prevails, see the right panel of Fig. 2. We further observe that at  $J = 0$  the transition from the QSHI to the EI is still first order, whereas that from the EI to the BI is continuous.

### C. Phase diagrams

We summarize our DMFT results in the two  $U$  vs  $M$  phase diagrams at  $J > 0$  and  $J = 0$ , respectively, left and right panels in Fig. 3. In both cases, the noninteracting QSHI-BI transition point at  $M = 2$  transforms at weak coupling into a

critical line determined by the condition,

$$M_{\text{eff}} \equiv M + \frac{1}{4} \text{Tr} [\Gamma_{03} \Sigma(\omega = 0)] = 2,$$

where  $\Sigma(\omega)$  is the self-energy matrix. The critical line corresponds to a second-order phase transition up to a critical value of the interaction  $U_c$ . For  $U > U_c$ , the transition turns first order [22,23,52], thus, without crossing a Dirac-like gapless point.

For  $J > 0$  and large enough  $U$ , the ground state describes a high-spin Mott insulator. An extended EI region with the  $P_1$ -order parameter intrudes between the QSHI and the hs-MI, see Fig. 3(a). Remarkably, the EI phase entirely covers the discontinuous topological transition occurring between the BI and the QSHI. The transitions from either the BI or the QSHI to the EI are of first order, whereas the transition from the EI to the hs-MI is continuous.

At  $J = 0$ , we observe an EI region between the QSHI and the BI at small  $M < 0.5$ . The QSHI-to-EI and EI-to-BI transitions are, respectively, of first and second orders. For very large  $U$ , the EI phase appears at  $M$  scaling as  $1/U$ . As we mentioned, the exciton condensate with order-parameter  $P_0$ , breaking  $C_4$ , and inversion symmetries for very small  $M$ , whereas for larger values, the order-parameter  $P_1$  prevails, breaking inversion, time-reversal, and spin  $U(1)$ . The transition between  $P_1$  and  $P_0$  is expected to be first order.

## III. MAGNETO-ELECTRIC NATURE OF THE EXCITONIC INSULATOR

In the EI phase with the  $P_1$ -order parameter, the breakdown of the symmetries protecting the nontrivial topology of the QSHI, i.e., time-reversal  $\mathcal{T}$ , inversion  $\mathcal{P}$ , and spin  $U(1)$  (yet not the product  $\mathcal{PT}$ ), dramatically changes the response to an electromagnetic field. Specifically, the triplet in-plane spin polarization nature of the excitonic-order parameter forbids a direct coupling to the electric field and, independently, to the magnetic field. However, the lack of both  $\mathcal{T}$  and  $\mathcal{P}$  symmetries allows the system to couple to the product of magnetic and electric fields, i.e., a linear magnetoelectric (ME) response [53]. Here, we show that the EI admits a finite ME susceptibility and, thus, corresponds to a ME insulator. Notably, this state should not be expected to be multiferroic because of the absence of magnetic and electric orders [53].

In order to study the ME properties, we evaluate the electric dipole response to a magnetic perturbation. Using Green's-Kubo formalism and neglecting vertex corrections, we obtain the following expression:

$$\Theta_{\mathbf{q}}^{ab}(v_m) = \sum_{\mathbf{k}, n} \frac{\text{Tr} [G(\mathbf{k}, i\omega_n) p^a(\mathbf{k}) G(\mathbf{k} + \mathbf{q}, i\omega_n + iv_m) M^b]}{\beta v_m}, \quad (7)$$

where  $a, b = 1, 2 \equiv x, y$  are the in-plane directions,  $M^a = \frac{1}{2} \Gamma_{a0}$  is the  $a$  component of the spin operator,  $p^a(\mathbf{k})$  is the momentum operator along  $a$ ,  $i\omega_n$ , and  $iv_m$  are, respectively, fermionic and bosonic Matsubara frequencies and

$$G(\mathbf{k}, i\omega_n) = [i\omega_n + \mu - H(\mathbf{k}) - \Sigma(i\omega_n)]^{-1}$$

is the interacting Green's function matrix. Given the multiorbital nature of the Hamiltonian (2), the momentum operator

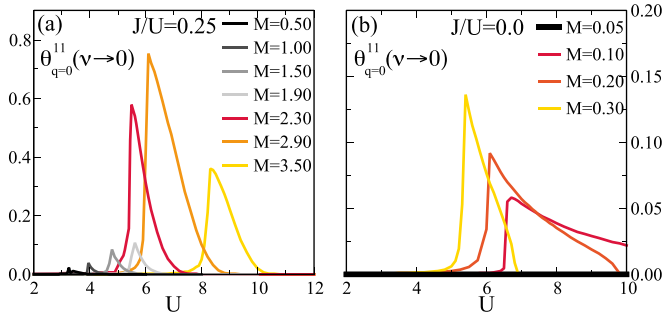


FIG. 4. Static and uniform limit of the magnetic-electric susceptibility as a function of the interaction strength  $U$  across the exciton phase transition. Data are for different values of  $M$  as indicated in the panels and for (a)  $J/U = 0.25$  and (b)  $J/U = 0.00$ .

should be evaluated using a generalized Peierls approximation [54–59]. The latter includes additional contributions, stemming from on-site interorbital processes that are dipole allowed. Specifically,

$$p_{\alpha\beta}^a(\mathbf{k}) = \partial^a H_{\alpha\beta}(\mathbf{k}) + i\Omega_{\alpha\beta}(\mathbf{k})d^a,$$

where  $\Omega^{\alpha\beta}(\mathbf{k}) = [E_\alpha(\mathbf{k}) - E_\beta(\mathbf{k})]$ ,  $E_\alpha(\mathbf{k})$  are the eigenvalues of the noninteracting Hamiltonian (2), and  $\vec{d} = (\Gamma_{02}, \Gamma_{32})$  is the dipole operator.

In the following, we consider the static  $\nu \rightarrow 0$ , and uniform  $\mathbf{q} = 0$  limit of the ME susceptibility. Our results are presented in Fig. 4 where we show the evolution of  $\Theta_{\mathbf{q}=0}^{11}(\nu = 0)$  as a function of  $U$  for finite and zero values of  $J$ . Since the contribution of the group velocity  $\partial_{k_\alpha} H_{\alpha\beta}(\mathbf{k})$  vanishes by symmetry, the ME response is entirely determined by the intra-atomic dipole transitions, which have finite expectation values in the EI phase. Indeed,  $\Theta_{\mathbf{q}=0}^{11}$  is finite only within the EI phase and vanishes otherwise. The magnetoelectric susceptibility shows the same dome structure of the order-parameter  $P_1$  as a function of  $U$ . The results at  $J = 0$  reported in Fig. 4(b) point out that the ME response vanishes when  $P_0 \neq 0$  as expected by symmetry. In the EI phase with  $P_1 \neq 0$ , the ME susceptibility is finite, and its peak value shifts to lower  $U$  with increasing  $M$ .

At  $J > 0$ , see Fig. 4(a), we observe a substantial change in the magnitude of the ME response. For  $M < 2$ , thus, starting from the QSHI, the susceptibility is globally small, whereas for larger  $M$ , the weight of  $\Theta_{\mathbf{q}=0}^{11}$  increases with seven times larger peak values. Remarkably, for any given  $J$  the largest ME response is reached in the proximity of the quantum critical point, which without allowing for  $P_1 \neq 0$  separates the continuous from the first-order topological quantum phase transition [22,24].

#### IV. SLAB GEOMETRY AND EDGE STATES

Finally, we explore the evolution across the QSHI-to-EI phase transition at  $J > 0$  in a slab geometry, i.e., with open boundary conditions along, say, the  $y$  axis, and periodic in the perpendicular direction. In this geometry, the electrons at the boundary experience an effectively larger interaction strength because of the reduced coordination. This effect becomes detectable near the phase transition. In the top panel

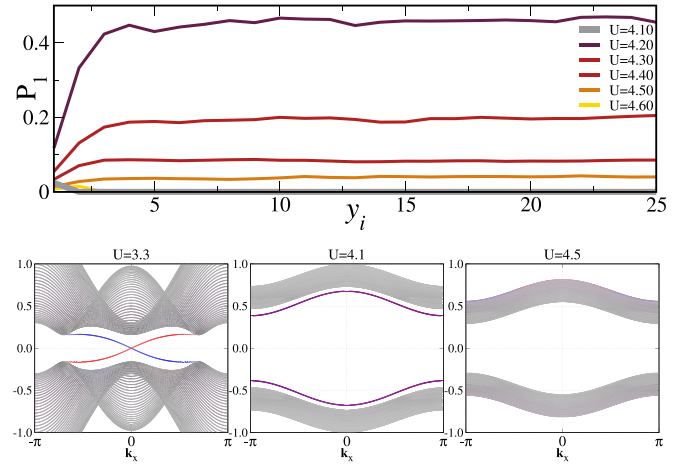


FIG. 5. Top panel: Excitonic-order parameter profile as a function of the site index along the  $y$  axis and across the QSHI to the EI transition. Bottom panels: Evolution of the low-energy band structure across the QSHI to the EI transition. Data are for a slab geometry with periodic boundary conditions along the  $x$  and open along the  $y$  axis with  $L_y = 50$  sites. Other model parameters are  $M = 1$  and  $J = 0.25U$ .

of Fig. 5, we show the evolution of the  $P_1$ -order parameter across the QSHI-EI first-order transition with  $M = 1$ . Before the transition, a finite value of the order parameter appears at the boundary and fast decays in the bulk interior. This behavior is akin to a wetting phenomenon [60,61]. Indeed, the first-order phase transition between QSHI and EI entails phase coexistence, namely, that both insulators can be minima of the free energy, although one of them is the global minimum, and the other just a local one.

Suppose that the QSHI is the thermodynamic stable phase. At the surface, the effective correlation strength is enhanced. It follows that if the system is not too far from the first-order transition, the surface can seed the nucleation of a wetting layer made by the metastable excitonic insulator. Depending on the static dielectric constants of the topological insulator  $\epsilon_{\text{QSHI}}$  and of the excitonic one  $\epsilon_{\text{EI}}$ , theory predicts partial or total wetting if, respectively,  $\epsilon_{\text{QSHI}} < \epsilon_{\text{EI}}$  or vice versa [62–65]. Since the order parameter (6) is not directly coupled to the electric field, and the gap grows across the QSHI-to-EI transition, we expect  $\epsilon_{\text{QSHI}} > \epsilon_{\text{EI}}$ , and, thus, total wetting. If that is indeed the case, we predict that the surface of a sufficiently correlated QSH insulator may be wet by a layer of excitonic insulator, lacking edge states but displaying magnetoelectricity, whose depth grows and diverges at the first-order transition.

Increasing  $U$  above the value of the bulk transition drives the sudden formation of a finite-order parameter throughout the whole sample as expected for a first-order transition. In this case, the order parameter near the boundary is instead reduced with respect to the bulk, consistently with the behavior of  $P_1$  vs  $U$  for  $M < 2$ , see the left panel in Fig. 2.

Further insights can be gained investigating the fate of the helical edge states, see the bottom panels of Fig. 5. The plots show the low-energy electronic band structure of the interacting system across the QSHI-to-EI transition. At small

coupling  $U = 3.3$ , well inside the QSHI (left panel), gapless helical edge states well separated from the bulk spectrum are visible. However, at  $U = 4.1$  (middle panel), where the bulk is still a QSHI but an EI wetting layer has formed, see the top panel of Fig. 5, edge states still exist but are gapped. On the contrary, for  $U = 4.5$  (right panel) where also the bulk is an EI, the edge states have disappeared inside the bulk continuum.

## V. CONCLUSIONS

In conclusion, we have investigated a canonical model of interacting quantum spin Hall insulators and showed that for a strong enough electronic correlation the system gets generally unstable towards an excitonic insulator that breaks time-reversal and inversion symmetries as well as the residual spin  $U(1)$  rotations. This state further evolves into a magnetic Mott insulator upon increasing the interaction strength where in-

version and spin- $U(1)$  symmetry are recovered. We explicitly show that the excitonic insulator has nonzero magnetoelectric susceptibility and, thus, is a good candidate platform for the realization of correlated multiferroic materials. Another remarkable phenomenon that we uncovered is the possible existence of an excitonic insulator wetting layer in a quantum spin Hall insulator.

## ACKNOWLEDGMENTS

A.A., M.C., and M.F. acknowledge support from H2020 Framework Programme under ERC Advanced Grant No. 692670 FIRSTORM. A.A. and M.C. also acknowledge support from Italian MIUR through PRIN2017 CEnTral (Protocol No. 20172H2SC4). A.A. was supported by the National Quantum Science and Technology Institute-NQSTI. G.M. was supported by the Swiss FNS/SNF through an Ambizione Grant.

- 
- [1] X.-L. Qi and S.-C. Zhang, Topological insulators and superconductors, *Rev. Mod. Phys.* **83**, 1057 (2011).
- [2] X.-G. Wen, Colloquium: Zoo of quantum-topological phases of matter, *Rev. Mod. Phys.* **89**, 041004 (2017).
- [3] B. A. Bernevig, T. L. Hughes, and S.-C. Zhang, Quantum spin hall effect and topological phase transition in HgTe quantum wells, *Science* **314**, 1757 (2006).
- [4] M. König, S. Wiedmann, C. Brüne *et al.*, Quantum spin hall insulator state in HgTe quantum wells, *Science* **318**, 766 (2007).
- [5] D. Hsieh, D. Qian, L. Wray, Y. Xia, Y. S. Hor, R. J. Cava, and M. Z. Hasan, A topological Dirac insulator in a quantum spin Hall phase, *Nature (London)* **452**, 970 (2008).
- [6] D. Hsieh, Y. Xia, L. Wray, D. Qian, A. Pal, J. H. Dil, J. Osterwalder, F. Meier, G. Bihlmayer, C. L. Kane, Y. S. Hor, R. J. Cava, and M. Z. Hasan, Observation of unconventional quantum spin textures in topological insulators, *Science* **323**, 919 (2009).
- [7] H. Zhang, C.-X. Liu, X.-L. Qi, X. Dai, Z. Fang, and S.-C. Zhang, Topological insulators in  $\text{Bi}_2\text{Se}_3$ ,  $\text{Bi}_2\text{Te}_3$  and  $\text{Sb}_2\text{Te}_3$  with a single Dirac cone on the surface, *Nat. Phys.* **5**, 438 (2009).
- [8] Y. L. Chen, J. G. Analytis, J.-H. Chu, Z. K. Liu, S.-K. Mo, X. L. Qi, H. J. Zhang, D. H. Lu, X. Dai, Z. Fang, S. C. Zhang, I. R. Fisher, Z. Hussain, and Z.-X. Shen, Experimental realization of a three-dimensional topological insulator,  $\text{Bi}_2\text{Te}_3$ , *Science* **325**, 178 (2009).
- [9] M. Kargarian and G. A. Fiete, Topological Crystalline Insulators in Transition Metal Oxides, *Phys. Rev. Lett.* **110**, 156403 (2013).
- [10] I. F. Herbut and L. Janssen, Topological Mott Insulator in Three-Dimensional Systems with Quadratic Band Touching, *Phys. Rev. Lett.* **113**, 106401 (2014).
- [11] X. Qian, J. Liu, L. Fu, and J. Li, Quantum spin hall effect in two-dimensional transition metal dichalcogenides, *Science* **346**, 1344 (2014).
- [12] B. Sun, W. Zhao, T. Palomaki, Z. Fei, E. Runburg, P. Malinowski, X. Huang, J. Cenker, Y.-T. Cui, J.-H. Chu, X. Xu, S. S. Ataei, D. Varsano, M. Palummo, E. Molinari, M. Rontani, and D. H. Cobden, Evidence for equilibrium exciton condensation in monolayer  $\text{WTe}_2$ , *Nat. Phys.* **18**, 94 (2022).
- [13] Y. Jia, P. Wang, C.-L. Chiu, Z. Song, G. Yu, B. Jäck, S. Lei, S. Klemenz, F. A. Cevallos, M. Onyszczak, N. Fishchenko, X. Liu, G. Farahi, F. Xie, Y. Xu, K. Watanabe, T. Taniguchi, B. A. Bernevig, R. J. Cava, L. M. Schoop *et al.*, Evidence for a monolayer excitonic insulator, *Nat. Phys.* **18**, 87 (2022).
- [14] N. Hao and J. Hu, Topological Phases in the Single-Layer Fese, *Phys. Rev. X* **4**, 031053 (2014).
- [15] N. Hao and S.-Q. Shen, Topological superconducting states in monolayer  $\text{FeSe}/\text{SrTiO}_3$ , *Phys. Rev. B* **92**, 165104 (2015).
- [16] Z. Wang, P. Zhang, G. Xu, L. K. Zeng, H. Miao, X. Xu, T. Qian, H. Weng, P. Richard, A. V. Fedorov, H. Ding, X. Dai, and Z. Fang, Topological nature of the  $\text{FeSe}_{0.5}\text{Te}_{0.5}$  superconductor, *Phys. Rev. B* **92**, 115119 (2015).
- [17] D. Wang, L. Kong, P. Fan, H. Chen, S. Zhu, W. Liu, L. Cao, Y. Sun, S. Du, J. Schneeloch, R. Zhong, G. Gu, L. Fu, H. Ding, and H.-J. Gao, Evidence for majorana bound states in an iron-based superconductor, *Science* **362**, 333 (2018).
- [18] L. Chen, H. Liu, C. Jiang, C. Shi, D. Wang, G. Cui, X. Li, and Q. Zhuang, Topological edge states in high-temperature superconducting  $\text{FeSe}/\text{SrTiO}_3$  films with Te substitution, *Sci. Rep.* **9**, 4154 (2019).
- [19] S. Rachel, Interacting topological insulators: A review, *Rep. Prog. Phys.* **81**, 116501 (2018).
- [20] Y. Zhang, Y. Ran, and A. Vishwanath, Topological insulators in three dimensions from spontaneous symmetry breaking, *Phys. Rev. B* **79**, 245331 (2009).
- [21] P. Dmytro and B. Leon, Mott physics and band topology in materials with strong spin-orbit interaction, *Nat. Phys.* **6**, 376 (2010).
- [22] A. Amaricci, J. C. Budich, M. Capone, B. Trauzettel, and G. Sangiovanni, First-Order Character and Observable Signatures of Topological Quantum Phase Transitions, *Phys. Rev. Lett.* **114**, 185701 (2015).
- [23] B. Roy, P. Goswami, and J. D. Sau, Continuous and discontinuous topological quantum phase transitions, *Phys. Rev. B* **94**, 041101(R) (2016).

- [24] A. Amaricci, J. C. Budich, M. Capone, B. Trauzettel, and G. Sangiovanni, Strong correlation effects on topological quantum phase transitions in three dimensions, *Phys. Rev. B* **93**, 235112 (2016).
- [25] L. Crippa, A. Amaricci, N. Wagner, G. Sangiovanni, J. C. Budich, and M. Capone, Nonlocal annihilation of weyl fermions in correlated systems, *Phys. Rev. Res.* **2**, 012023(R) (2020).
- [26] J. C. Budich, B. Trauzettel, and P. Michetti, Time Reversal Symmetric Topological Exciton Condensate in Bilayer HgTe Quantum Wells, *Phys. Rev. Lett.* **112**, 146405 (2014).
- [27] J. Kuneš, Excitonic condensation in systems of strongly correlated electrons, *J. Phys.: Condens. Matter* **27**, 333201 (2015).
- [28] D. Geffroy, J. Kaufmann, A. Hariki, P. Gunacker, A. Hausoel, and J. Kuneš, Collective Modes in Excitonic Magnets: Dynamical Mean-Field Study, *Phys. Rev. Lett.* **122**, 127601 (2019).
- [29] G. Mazza, M. Rösner, L. Windgätter, S. Latini, H. Hübener, A. J. Millis, A. Rubio, and A. Georges, Nature of Symmetry Breaking at the Excitonic Insulator Transition: Ta<sub>2</sub>NiSe<sub>5</sub>, *Phys. Rev. Lett.* **124**, 197601 (2020).
- [30] A. Blason and M. Fabrizio, Exciton topology and condensation in a model quantum spin hall insulator, *Phys. Rev. B* **102**, 035146 (2020).
- [31] L. Windgätter, M. Rösner, G. Mazza, H. Hübener, A. Georges, A. J. Millis, S. Latini, and A. Rubio, Common microscopic origin of the phase transitions in Ta<sub>2</sub>NiS<sub>5</sub> and the excitonic insulator candidate Ta<sub>2</sub>NiSe<sub>5</sub>, *npj Comput. Mater.* **7**, 210 (2021).
- [32] G. Mazza and A. Amaricci, Strongly correlated exciton-polarons in twisted homobilayer heterostructures, *Phys. Rev. B* **106**, L241104 (2022).
- [33] D. Varsano, M. Palummo, E. Molinari, and M. Rontani, A monolayer transition-metal dichalcogenide as a topological excitonic insulator, *Nat. Nanotechnol.* **15**, 367 (2020).
- [34] M. Dzero, K. Sun, V. Galitski, and P. Coleman, Topological Kondo Insulators, *Phys. Rev. Lett.* **104**, 106408 (2010).
- [35] M. Dzero, K. Sun, P. Coleman, and V. Galitski, Theory of topological Kondo insulators, *Phys. Rev. B* **85**, 045130 (2012).
- [36] X. Zhang, N. P. Butch, P. Syers, S. Ziemak, R. L. Greene, and J. Paglione, Hybridization, Inter-Ion Correlation, and Surface States in the Kondo Insulator SmB<sub>6</sub>, *Phys. Rev. X* **3**, 011011 (2013).
- [37] F. Lu, J. Z. Zhao, H. Weng, Z. Fang, and X. Dai, Correlated Topological Insulators with Mixed Valence, *Phys. Rev. Lett.* **110**, 096401 (2013).
- [38] J. Knolle and N. R. Cooper, Excitons in Topological Kondo Insulators: Theory of Thermodynamic and Transport Anomalies in smb<sub>6</sub>, *Phys. Rev. Lett.* **118**, 096604 (2017).
- [39] A. Georges, G. Kotliar, W. Krauth, and M. J. Rozenberg, Dynamical mean-field theory of strongly correlated fermion systems and the limit of infinite dimensions, *Rev. Mod. Phys.* **68**, 13 (1996).
- [40] W. Metzner and D. Vollhardt, Correlated Lattice Fermions in  $d = \infty$  Dimensions, *Phys. Rev. Lett.* **62**, 324 (1989).
- [41] E. Müller-Hartmann, Correlated fermions on a lattice in high dimensions, *Z. Phys. B* **74**, 507 (1989).
- [42] D. Geffroy, A. Hariki, and J. Kuneš, Excitonic magnet in external field: Complex order parameter and spin currents, *Phys. Rev. B* **97**, 155114 (2018).
- [43] C. A. F. Vaz, J. Hoffman, C. H. Ahn, and R. Ramesh, Magnetoelectric coupling effects in multiferroic complex oxide composite structures, *Adv. Mater.* **22**, 2900 (2010).
- [44] F. Thöle, A. Keliri, and N. A. Spaldin, Concepts from the linear magnetoelectric effect that might be useful for antiferromagnetic spintronics, *J. Appl. Phys.* **127**, 213905 (2020).
- [45] A. Amaricci, L. Crippa, A. Scazzola, F. Petocchi, G. Mazza, L. de Medici, and M. Capone, Edipack: A parallel exact diagonalization package for quantum impurity problems, *Comput. Phys. Commun.* **273**, 108261 (2022).
- [46] S. Miyakoshi and Y. Ohta, Antiferromagnetic topological insulator state in the correlated bernevig-hughes-zhang model, *Phys. Rev. B* **87**, 195133 (2013).
- [47] L. Wang, X. Dai, and X. C. Xie, Interaction-induced topological phase transition in the Bernevig-Hughes-Zhang model, *Europhys. Lett.* **98**, 57001 (2012).
- [48] T. Yoshida, S. Fujimoto, and N. Kawakami, Correlation effects on a topological insulator at finite temperatures, *Phys. Rev. B* **85**, 125113 (2012).
- [49] J. C. Budich, R. Thomale, G. Li, M. Laubach, and S.-C. Zhang, Fluctuation-induced topological quantum phase transitions in quantum spin-Hall and anomalous-Hall insulators, *Phys. Rev. B* **86**, 201407(R) (2012).
- [50] A. Amaricci, A. Valli, G. Sangiovanni, B. Trauzettel, and M. Capone, Coexistence of metallic edge states and antiferromagnetic ordering in correlated topological insulators, *Phys. Rev. B* **98**, 045133 (2018).
- [51] P. Werner and A. J. Millis, High-Spin to Low-Spin and Orbital Polarization Transitions in Multiorbital Mott Systems, *Phys. Rev. Lett.* **99**, 126405 (2007).
- [52] G. Mazza, A. Amaricci, M. Capone, and M. Fabrizio, Field-Driven Mott Gap Collapse and Resistive Switch in Correlated Insulators, *Phys. Rev. Lett.* **117**, 176401 (2016).
- [53] W. Eerenstein, N. D. Mathur, and J. F. Scott, Multiferroic and magnetoelectric materials, *Nature (London)* **442**, 759 (2006).
- [54] M. Cruz, M. R. Beltrán, C. Wang, J. Tagüeña-Martínez, and Y. G. Rubo, Supercell approach to the optical properties of porous silicon, *Phys. Rev. B* **59**, 15381 (1999).
- [55] T. G. Pedersen, K. Pedersen, and T. B. Kriestensen, Optical matrix elements in tight-binding calculations, *Phys. Rev. B* **63**, 201101(R) (2001).
- [56] J. M. Tomczak and S. Biermann, Optical properties of correlated materials: Generalized peierls approach and its application to vo<sub>2</sub>, *Phys. Rev. B* **80**, 085117 (2009).
- [57] P. Wissgott, J. Kuneš, A. Toschi, and K. Held, Dipole matrix element approach versus peierls approximation for optical conductivity, *Phys. Rev. B* **85**, 205133 (2012).
- [58] G. Mazza and A. Georges, Superradiant Quantum Materials, *Phys. Rev. Lett.* **122**, 017401 (2019).
- [59] J. Li, D. Golez, G. Mazza, A. J. Millis, A. Georges, and M. Eckstein, Electromagnetic coupling in tight-binding models for strongly correlated light and matter, *Phys. Rev. B* **101**, 205140 (2020).
- [60] P. G. de Gennes, Wetting: Statics and dynamics, *Rev. Mod. Phys.* **57**, 827 (1985).
- [61] D. Bonn, J. Eggers, J. Indekeu, J. Meunier, and E. Rolley, Wetting and spreading, *Rev. Mod. Phys.* **81**, 739 (2009).

- [62] I. E. Dzyaloshinskii, E. M. Lifshitz, and L. P. Pitaevskii, General theory of van der waals' forces, *Sov. Phys. Usp.* **4**, 153 (1961).
- [63] Y. S. Barash and V. L. Ginzburg, Electromagnetic fluctuations in matter and molecular (van-der-waals) forces between them, *Sov. Phys. Usp.* **18**, 305 (1975).
- [64] R. Lipowsky, Upper Critical Dimension for Wetting in Systems with Long-Range Forces, *Phys. Rev. Lett.* **52**, 1429 (1984).
- [65] L. Del Re, M. Fabrizio, and E. Tosatti, Nonequilibrium and non-homogeneous phenomena around a first-order quantum phase transition, *Phys. Rev. B* **93**, 125131 (2016).